

IN-FLIGHT CuZrTiNi PARTICLE ENERGY TAILORING IN KINETIC SPRAYING DEPOSITION

Juneseob Kim¹, Sanghoon Yoon¹, Hanshin Choi², Hwijun Kim², Hyungho Jo²
and Changhee Lee¹

¹Kinetic Spray Coating Laboratory(NRL), Division of Materials Science & Engineering, Hanyang University, Seoul, Korea

²Nanomaterial Team, Korea Institute of Industrial Technology, Incheon, Korea

Received: March 29, 2008

Abstract. Inert gas atomized CuZrTiNi bulk metallic glass powders were sprayed onto mild steel substrates by kinetic spraying with powder carrier gas temperatures of RT, 450 °C (within the supercooled liquid region), and 550 °C (above the crystallization temperature). The microstructure, porosity, micro hardness, and bond strength of the as-sprayed coatings were characterized as a function of the powder carrier gas temperature. With the increase of powder carrier gas temperature, the crystal phase fraction also increased with grain growth. The brittle nature of the crystal phase and poor contact nature resulted in a lower bond strength of the BMG coating which was produced at the powder carrier gas temperature of 550 °C.

1. INTRODUCTION

Bulk metallic glass (BMG) materials have shown unique features, and thus there has been much research into the application of their high hardness and corrosion potential for engineering components. However, high yield strength and low ductility make it impossible to deform the BMG materials at low temperatures [1-3]. Therefore, most of the research concerning the deformation of BMG materials has attempted to utilize superplasticity [4]. Owing to the instability of the amorphous phase, irreversible amorphous to crystalline phase transformation occurs when the applied thermal cycle is inadequate. In accordance with the phase instability, and also the glass forming ability of BMG materials, coatings may be a potent alternative for industrial applications [5,6].

In this study, CuZrTiNi BMG coatings were overlaid onto mild steel substrates by kinetic spraying. During the high velocity particle impactation, impacting particle deformation undergoes an abnormally

high strain rate of up to 10^9 s⁻¹, and the deformation behavior is affected by the impacting particle velocity, mass, density, shape, thermophysical, and thermo-mechanical properties. It is well-known that BMG materials show temperature and strain rate dependent superplasticity, and most engineering processes have tried to utilize the sudden decrease of viscosity of BMG within the supercooled liquid region. For this reason, the initial temperature of impacting particles has a critical influence on the deformation behavior. Therefore, by using a kinetic spraying system that alters the powder carrier gas temperature, the impacting BMG particle temperature was changed, and the resulting coating properties were investigated.

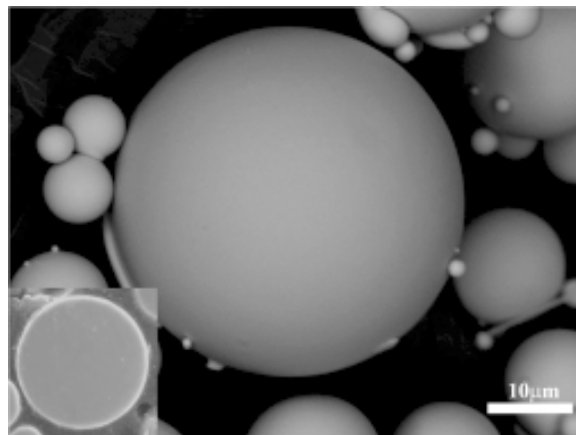
2. EXPERIMENTAL PROCEDURE

CuZrTiNi bulk metallic glass feedstock with a composition of 54 at.% Cu, 22 at.% Zr, 18 at.% Ti, and 6 at.% Ni produced by using gas atomization. The characteristics of CuZrTiNi bulk metallic glass feed-

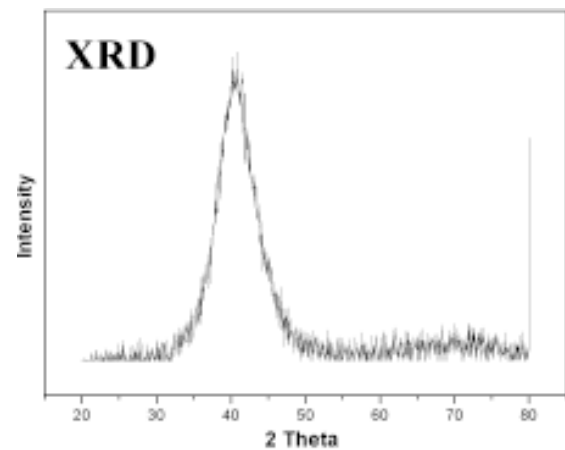
Corresponding author: Changhee Lee, e-mail: chlee@hanyang.ac.kr

Table 1. Process parameters.

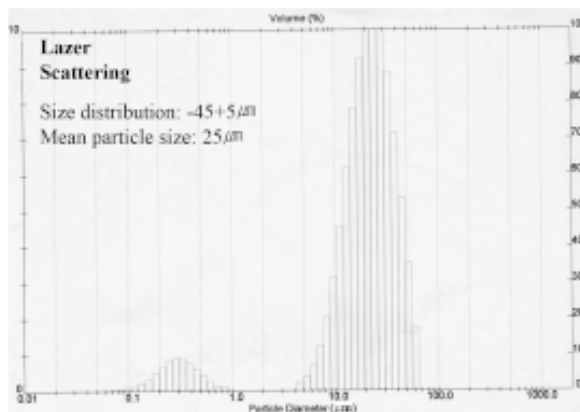
Gas	Process gas pressure	Process gas temperature	Pre-heating Temperature
Helium	2.9 MPa	550 °C	RT, 450 °C, 550 °C



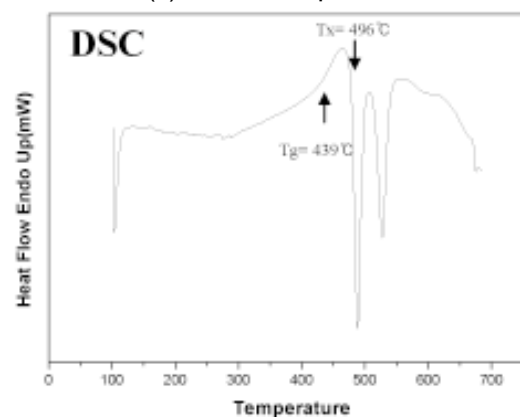
(a) Morphology



(c) Phase composition

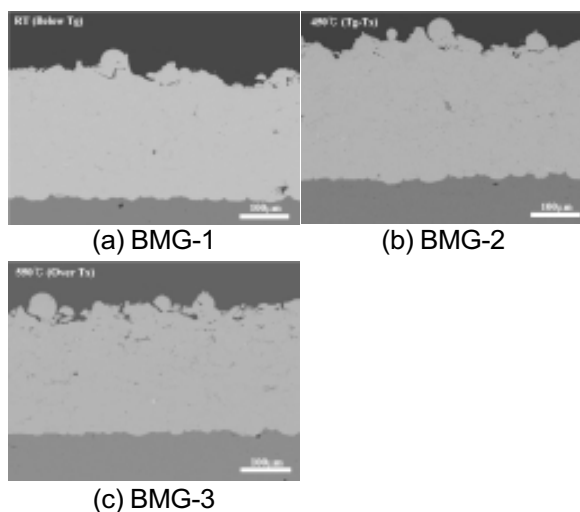


(b) Size distribution

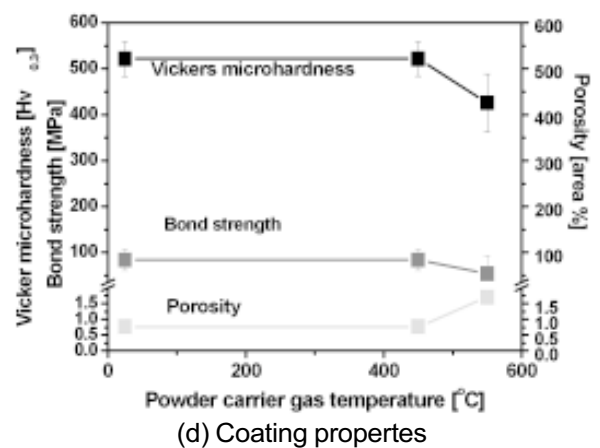


(d) Thermal properties

Fig. 1. Characteristics of CuZrTiNi bulk metallic glass feedstock.



(c) BMG-3



(d) Coating properties

Fig. 2. Cross-sectional coating morphology and coating properties (Vickers microhardness, bond strength, and porosity) of as-sprayed coatings as a function of the powder carrier gas temperature.

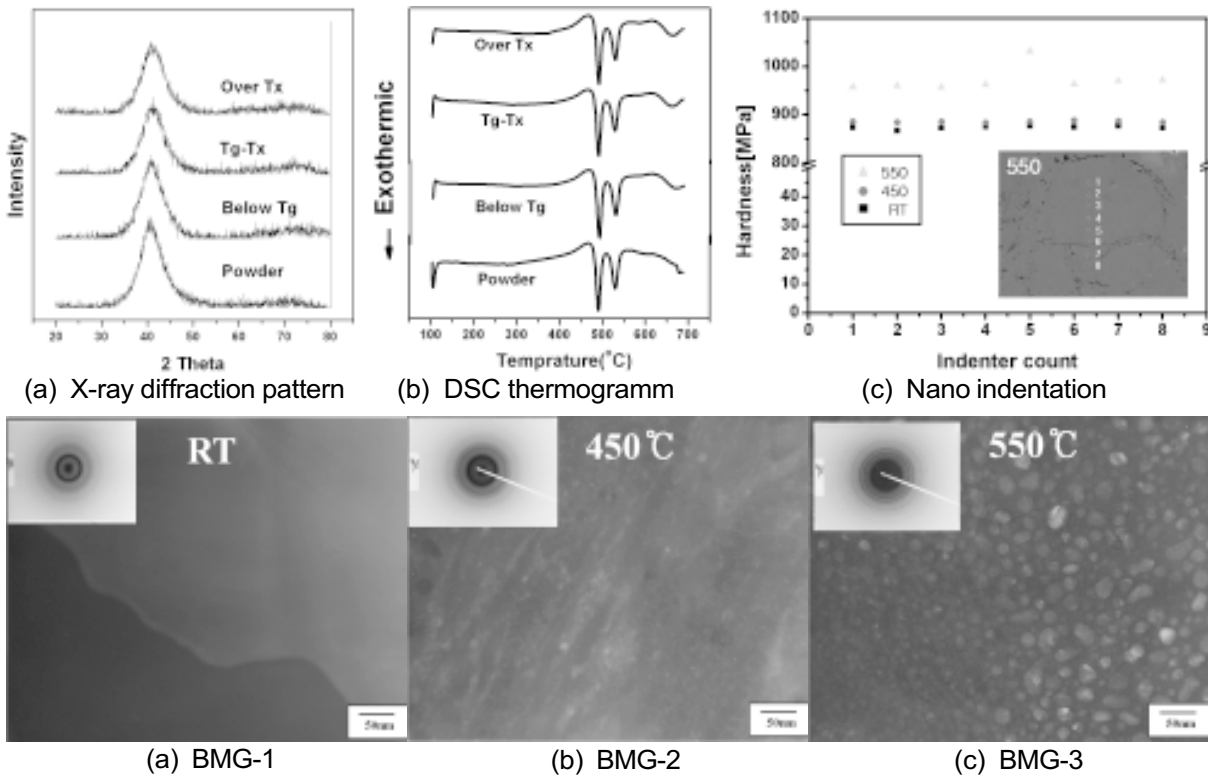


Fig. 3. XRD, DSC, TEM analysis (bright field image and SAD pattern) and nano-indentation results for the as-sprayed coatings.

stock and process parameters are listed in Table 1 and Fig. 1. This experiment used a de Laval nozzle. Helium gas was used for the process gas. Nitrogen gas was used for the powder carrier gas. The plane-view and cross sections of the macroscopic and microscopic structures were observed.

The properties of as-sprayed BMG coatings were observed by using X-ray diffractometry and differential scanning calorimetry. In-flight particle oxidation was evaluated by measuring oxygen content in both feedstock and coatings using a LECO N/O test. To measure the bond strength of coating/substrate, the Stud Pull Coating Adherence Test was carried out by using a Romulus Bond Strength Tester.

3. RESULTS AND DISCUSSION

The cross-sectional microstructure, porosity, Vickers microhardness, and bond strength of as-sprayed CuZrTiNi BMG coatings are shown in Fig. 2. The effects of the powder carrier gas temperature on the as-sprayed BMG coating characteristics show a transition at 450 °C. From RT to 450

°C, there are no marked differences in coating microstructure, microhardness, and bond strength, though slight increases in coating thickness and microhardness are observed. For bond strength, failures for both BMG-1(RT) and BMG-2(T_g - T_x) occurred at the interface between the epoxy and coating surface, and thus any difference in bond strength between them is meaningless. However, the porosity within the BMG-3 (higher than T_x) coating was markedly increased with notable decreases of micro-hardness and bond strength. In addition, the BMG-3 coating showed adhesive failure. In order to clarify the dependence of the coating characteristics on the powder carrier gas temperature, phase identification was conducted as shown in Figs. 3a and 3b. They all contain a diffuse halo peak without any marked crystalline phase diffraction. For thermal properties, as-sprayed coatings as well as powder feedstock apparently show the same double step crystallization behavior. However, the amorphous phase fraction decreased with the increase of powder carrier gas temperature (98% for BMG-1, 95% for BMG-2, and 92% for BMG-3)

when the crystallinity of as-sprayed coatings was quantified by the ratio of crystallization enthalpy of each coating to that of the powder feedstock. To identify the crystallization of BMG particles, TEM analysis and nano-indentation tests were conducted [Fig. 3]. As shown in the bright field image and corresponding selected area diffraction pattern, the phase fraction and grain size increased when the powder carrier gas temperature was raised. In addition, nano-indentation using a Berkovich indent was conducted from the center region of a splat to that of a neighboring splat as shown in Fig. 3c. The nano-hardness distribution in the BMG-2 coating was similar to that of BMG-1, but a slightly higher hardness value was observed in BMG-2. In the case of BMG-3, markedly higher nano-hardness values than the other coatings were observed, as well as a sharp increase in the nano-hardness near the splat boundary, which is a characteristic feature of BMG-3. It could be deduced that the crystallization of as-sprayed BMG coatings was affected by the powder carrier gas temperature, and that the resulting crystallinity of the as-sprayed coatings had critical influences on coating microstructure, microhardness, and bond strength. Marked increases of the crystalline phase fraction and grain size were identified by both TEM analysis and nano-indentation. Moreover, the higher crystalline phase fraction could be assumed by the sharp increase in nano-hardness near the splat boundary of BMG-3. In summary, the transition of microstructure and bond strength of BMG-3 could be explained by the powder carrier gas temperature and impacting behavior. After a BMG particle is injected into hot gas dynamics, the particle continuously interacts with the gas dynamics via momentum transfer and heat transfer. Thus, the in-flight particle temperature is higher when the gas temperature is increased, even though the gas dynamic temperature is markedly changed due to the thermal inertia. When the particle is impacted, strain hardening usually competes with thermal softening, and adiabatic shear instability affects the splat formation. Therefore, more intimate contact can be expected with an increased initial temperature of the impacting particle for conventional engineering metals. However, the thermal cycle of an impacting particle should be considered, because an improper thermal cycle causes BMG particles to undergo irreversible crystallization due to the inherent phase instability of the amorphous phase. As a result, increased powder carrier gas

temperature creates for the particles a more susceptible thermal cycle during impact (i.e. higher initial temperature and increased heat generation caused by severe deformation), resulting in higher crystallinity of the impacted splat. Subsequently, particle impacts on the crystallized BMG splat and the brittle nature of crystallized BMG creates fractures at the impacting surface. This may explain the higher porosity observed in BMG-3. Owing to the higher porosity and higher crystallinity, BMG-3 showed lower bonding strength.

4. CONCLUSION

In this study, the effects of powder carrier gas temperature on the coating microstructures and coating properties were investigated. As the powder carrier gas temperature was increased, the crystal phase fraction increased with an increase of grain size. The increase of crystallinity of BMG coatings seemed to result from the increase of the initial temperature of impacting particles. The brittle nature of crystallized BMG produced fractures of the impacting surface during splat formation with the increased impacting particle temperature, though conventional metallic particles showed more intimate contact at higher impacting particle temperature. Accordingly, the higher porosity and brittle nature of partially crystallized BMG coatings showed lower bonding strength.

ACKNOWLEDGEMENTS

This work was supported by the Korea Science and Engineering Foundation (KOSEF) grant funded by the Korea government(MOST) (No.2006-02289).

REFERENCES

- [1] D. Fatay, J. Gubicaza, P. Szommer, J. Lendvai, M. Blétry and P. Guyot // *Mater. Sci. and Eng. A* **387-389** (2004) 1001.
- [2] H.J. Kim, J.K. Lee, S.Y. Shin, H.G. Jeong, D.H. Kim and J.C. Bae // *Intermetallics* **12** (2004) 1109.
- [3] H.S. Kim // *Metal and Mater. International.* **10** (2004) 461.
- [4] Inoue A // *Acta Mater* **48** (2000) 279.
- [5] H.S Choi, S.H Yoon, G.Y Kim, H.H Jo and C. Lee // *Scripta Materialia* **53** (2005) 125.
- [6] S.H Yoon, C. Lee, H.S Choi and H.H Jo // *Materials Science and Engineering A* **415** (2006) 45.